Semiphenomenological model for the dispersion of DNA during electrophoresis in a microfluidic array of posts

Kevin D. Dorfman and Jean-Louis Viovy*
Laboratoire Physicochimie-Curie, CNRS/UMR 168, Institut Curie, 26 Rue d'Ulm, F-75248 Paris Cedex 5, France
(Received 8 September 2003; published 12 January 2004)

A lattice Monte Carlo model is proposed for quantifying the dispersion of DNA during microfluidic electrophoresis in a quasiperiodic array of posts similar to that encountered in the microfluidic self-assembly of magnetic bead columns. The transport model is semiphenomenological in the sense that all parameters, such as the post geometry, average collision time, and collision probability, are assumed to be accessible either directly from experiment or from a model of the microscale physics. Asymptotically exact formulas are obtained for the mean velocity and dispersivity using Taylor-Aris dispersion theory, which permits a straightforward analysis of the separation efficiency. The model is applicable to a variety of situations involving collision-retardation processes.

DOI: 10.1103/PhysRevE.69.011901 PACS number(s): 87.15.Tt, 05.40.Jc

I. INTRODUCTION

Characterizing the dynamics of DNA during its interaction with a post, in particular the dependence of the dynamics upon the length of the DNA strand, is requisite for properly quantifying many important separation processes. For conventional electrophoretic separations in gels, the DNA-post interaction represents a useful, albeit idealized, model for the entanglement of DNA with the otherwise randomly arranged fibers of the gel. In contrast, the DNA-post interaction very precisely models the prevailing separation mechanism in a number of microfluidic devices. Such devices typically exploit microlithography to fabricate perfectly periodic arrays of posts [1], and this has led to a number of experimental [2] and theoretical [3–8] analyses of DNA dynamics in such arrays. As an alternative to microlithographic fabrication, it is also possible to form periodic arrays of posts through the self-assembly of superparamagnetic beads, the ''Ephesia'' system [9].[1]

Although theoretical studies are typically motivated by applications involving arrays of posts, for the most part [3–7] they focus upon the intricate dynamics of the collision with a single isolated post. Thus, one hopes to arrive at a rational model for the average time engaged with the post (the trapping time), τ, and the collision probability Π_c as a function of the characteristics of the post and the size of the DNA. For practical applications, though, it is the *cumulative* effect of these post collisions which determines the average DNA motion and, ultimately, the separation efficiency. Moreover, it is not entirely obvious how to average single-post dynamics into relevant macroscopic quantities, such as the dispersion and the separation resolution.

This issue of homogenization can be side stepped entirely by resorting to detailed Brownian dynamics simulations of the DNA motion for a particular arrangement of posts [8]. In addition to quantifying the average transport through the array, detailed simulations may provide insight into the microscale dynamics, such as the relaxation (or lack thereof) of the DNA between post-collision events. However, large scale simulations are, by necessity, computationally intensive, and each simulation only reveals information about a single specific combination of experimental parameters. Consequently, the simple analytical theory proposed here, despite the fact that it may be less precise than a detailed simulation, is still of great utility because it produces parametric results.

In addition, semiphenomenological theories such as the one developed here are useful for conceptually understanding the separation process. Indeed, this has been the case in the past for several novel microfluidic protocols, such as those based upon rectified Brownian motion [10,11] and entropic trapping [12]. Naturally, initial analyses such as these focus upon the mobility difference arising in the device, since it is this difference which gives rise to the separation. However, completely characterizing the separation also requires knowledge of the dispersivity $\overline{D}^*$, which quantifies the separation sharpness. Unfortunately, the dispersivity often proves much more difficult to calculate than the average velocity $\overline{U}^*$. For example, intuition suggests that transport in an array of posts should yield a mean velocity of the form

$$\overline{U}^* = \frac{U}{1+K}, \tag{1.1}$$

where U is the velocity in the absence of the posts and K is a ''retardation factor,'' presumably calculable from the single-post data. As will be evident shortly, the proper quantification of $\overline{D}^*$ is not so obvious.

We present here a framework for properly averaging microscale post-collision data into simple analytical results for the average DNA mobility and dispersivity through the array. We focus upon a disordered staggered array of posts, a con-

*Electronic address: Jean-Louis.Viovy@curie.fr

[1]The term Ephesia refers to the temple of Artemis in ancient Greece (present day Turkey). The temple was constructed of an array of columns and repeatedly destroyed and reconstructed on the same site. Likewise, under the influence of an external magnetic field, the magnetic beads form periodic arrays of columns which can be reversibly assembled and disassembled in the same channel by turning the magnetic field on and off.

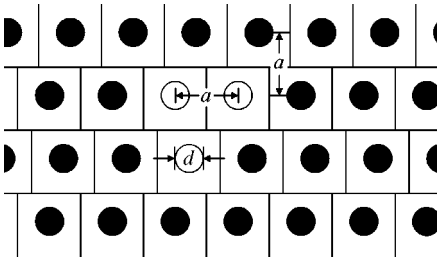

FIG. 1. Schematic of a quasiperiodic staggered array of cylindrical posts of diameter d and intrarow center-to-center spacing a. The rows of obstacles are separated by the distance a, but are randomly "shifted" to produce a configuration similar to that resulting from the self-assembly of magnetic bead columns.

figuration which is similar to that realized in the Ephesia system. Our approach to the transport phenomena is semiphenomenological, postulating that the average post spacing, the probability of colliding with a post, Π_c, and the average time to negotiate the post, τ, can be obtained experimentally or from a detailed microscale model. The mean velocity and dispersivity are then calculated exactly via generalized Taylor-Aris dispersion theory [13,14], without the need to resort to numerical simulations, and the implications of these results on the separation process are discussed. Although the model is developed in the context of post-collision induced separations, the generic results for $\overline{U}^*$ and $\overline{D}^*$ can be applied to many other experimentally relevant situations involving periodically retarded motion, such as entropic trapping [12] and spatially periodic ratchet-type separations, by specifying a particular model for Π_c and τ.

II. MODEL DESCRIPTION

We focus our attention on quasiperiodic arrays of posts, such as the one depicted in Fig. 1. Within a given row, the cylindrical posts of diameter d are regularly spaced by the distance a. The spacing between the center lines of adjacent rows is also a, but the alignment between the rows is disordered. The resulting array possesses the qualitative features of a staggered or hexagonal array, but without the strict periodicity. Such disorder is characteristic of the Ephesia system, in which repulsion between the magnetic posts leads to local order and a Bragg peak in the diffraction pattern, but interactions with the channel walls prevent long-range order.

In this discrete lattice Monte Carlo model, the motion of the DNA is approximated by jumps between the volume elements (lattice sites) represented by the boxes in Fig. 1. In the absence of any interactions with the post, the DNA jumps from site to site in the direction of the field with its free-solution velocity, $U=\mu_0 E$, where μ_0 is the free-solution mobility of the strand and E is the applied field. When arriving in one of the volume elements, we assume (i) the probability of encountering a post is quantified by the collision probability Π_c and (ii) if the DNA becomes hooked on the post, it is retained for an average time τ. A number of microscale models have been proposed for the latter parameters, and the details of these models will be discussed shortly. For the most part, though, we will employ τ and Π_c as model parameters in our calculations, in order to produce generic results which transcend the specifics of the underlying microscale model. At times we will adopt simple models for τ and Π_c when it aids in conceptual understanding, or when it allows us to predict general experimental trends.

The use of an average trapping time, rather than specifying a complete distribution of trapping times, is invoked for simplicity and supported by numerical simulations [3,5] which indicate that universal behavior exists for τ across a broad range of parameters. A particularly simple model for τ assumes that it scales with the inverse of the applied field, $\tau \sim E^{-1}$, which appears to be the case from single-post experiments [2] and scaling arguments [7] in relatively strong fields.

In a coarse-grained model such as the one developed here, the simplest possible model for the collision probability assumes a dependence only upon the linear post density d/a that the DNA sees in one dimension as it moves through the array. In a semiempirical comparison of this theory and Ephesia experiments [15], use of the latter collision probability furnished reasonable agreement for the band broadening. However, this purely geometric interpretation of Π_c is most likely an oversimplification, since simulation data [5,7] and recent experiments [16] suggest that the collision probability depends strongly upon the initial offset with the center of the post, the so-called "impact parameter," as well as the field strength [16]. Moreover, Brownian dynamics simulations [8] in sparse arrays with typical experimental post densities indicate that, for sufficiently dense arrays, the collision probability eventually *decreases* with increasing post density because the DNA do not have sufficient time to relax between encounters with the post. Finally, simulations [7] predict a coupling between the size of the posts, d, and the trapping time τ since it is difficult for short DNA to become extended around large obstacles. However, the latter coupling can be accounted for in a semiempirical manner [15] by using an experimentally measured trapping time.

A key feature of our model is the Markovian assumption that the collision probability is identical for all post regions. For perfectly staggered arrays, this is probably not a good assumption. After unhooking in a perfect array, the DNA is misaligned with the next post, and must reorient itself via molecular diffusion before it has the potential to suffer another collision. The characteristic time for this reorientation process, which can be much longer than the DNA relaxation time, implies that the collision probability increases as the DNA moves further away from its last collision, resulting in a non-Markovian process [5]. In contrast, the random relative location between successive posts in our quasiregular array lessens the correlation between the unhooking from the first post and the probability of colliding with the next one. In the present model, we assume that the shifted layers and resulting post randomness ensures complete decorrelation between collision events.

At first glance, it would appear that the issue of relaxation would severely limit the realism of our model for actual separations of long DNA. The time for the DNA to return to its equilibrium conformation is characterized by the Rouse relaxation time, $\tau_R \approx Nb^2/D$, where D is the diffusion coef-

ficient, b is the persistence length, and N is the number of persistence lengths. To ensure that the DNA is completely relaxed between possible collisions, τ_R must be longer than the mean transit time a/U between post regions. For λ-DNA, the Rouse relaxation time is of the order of seconds, which means that for a typical post spacing $a \sim 5$ μm and electrophoretic mobility $\mu_0 \sim 3$ μm V/cm s, we would be limited to fields $E < 0.2$ V/cm. However, immediately after engaging a post, there is a very rapid relaxation due to nonlinear elasticity [5], and recent experiments [16] indicate that much of the relaxation process for λ-DNA takes place in ≈ 0.15 s. Consequently, it is likely that the DNA have undergone significant relaxation before their next collision, even at relatively high fields. Actually, some level of ''relaxation memory'' between collisions could be taken into account in the model via reduced effective collision parameters. Avoiding this, however, reduces the number of free parameters in the model and increases its generality.

Owing to the strong fields typically employed in experiments (up to 35 V/cm) [15], we neglect longitudinal diffusion and lateral jumps due to molecular diffusion, thereby requiring that each jump results in motion in the direction of the field. This convective model should be reasonable when the reduced field is large [17], namely, when

$$\frac{\mu_0 E a}{2D} \gg 1. \tag{2.1}$$

With the values for μ_0 and a cited above and $D \sim 0.25$ μm^2/s, Eq. (2.1) requires that $E \gg 0.1$ V/cm, which is easily satisfied in experiments. This assumption is further supported by video microscopy experiments in the Ephesia system, which reveal that the DNA tends to traverse the array in a more-or-less linear fashion.

III. GENERALIZED TAYLOR-ARIS DISPERSION THEORY

In the present section, we use Taylor-Aris dispersion theory [13,14] to calculate the mean velocity $\overline{U}^*$ and dispersivity $\overline{D}^*$ from the model described above. This procedure entails two steps (i) converting the model into the local graph and specifying the transport thereon and (ii) computing $\overline{U}^*$ and $\overline{D}^*$ from the general theory.

A. Graphical construction

In each volume element of Fig. 1, the DNA can either engage the post or pass through the region unimpeded, and the entry into the volume element can be preceded either by an engagement with the post or by an unimpeded pass. Consequently, the lattice model can be represented by the spatially periodic (basic) graph depicted in Fig. 2(a). In this graph, engagements with the post correspond to the black circles h and unimpeded passes correspond to the white circles m, and the edges represent the possible transitions. By convention, the nodes i are represented by Roman characters and the edges j are represented by Arabic numerals.

In order to perform the calculation, it is necessary to extract from the model (i) the jump time T; (ii) the transition probabilities $w(j)$ for moving between the nodes of the lattice; and (iii) the probabilities $w(i)$ that the DNA does not exit node i during the time T. The neglect of translational diffusive effects renders this a convective model, whereupon jumps on the graph occur, on average, with the time step

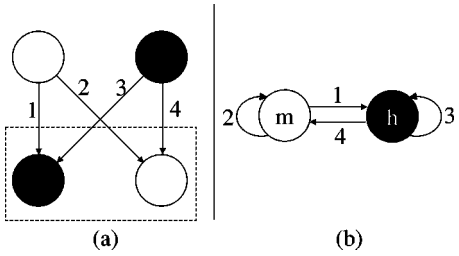

FIG. 2. (a) Basic graph for the array of posts depicted in Fig. 1. Open circles m and black circles h, respectively, correspond to ''misses'' and ''hits'' with the post. The edges numbered 1–4 correspond to the different types of jumps that can be made on the graph. The dashed box is the graphical equivalent of the volume elements of Fig. 1. (b) The local graph. Edges 2 and 3, which correspond to consecutive misses or hits, result in loops on the graph.

$$T = \frac{a}{U} = \frac{a}{\mu_0 E}. \tag{3.1}$$

If the DNA is resident on a nonpost node m, it must exit the node [i.e., $w(m)=0$] and can do so through the edges labeled 1 and 2. With the probability of hitting the post Π_c, the transition probabilities for exiting node m are $w(1) = \Pi_c$ and $w(2) = 1 - \Pi_c$. When the DNA has engaged the post on node h, the probability of remaining on the post, $w(h)$, is $1 - \alpha^{-1}$, where α is the dimensionless trapping time

$$\alpha \equiv \frac{\tau}{T}. \tag{3.2}$$

Accounting for the trapping time, the remaining transition probabilities are $w(3) = \Pi_c/\alpha$ and $w(4) = (1 - \Pi_c)/\alpha$. Implicit in this model is the fact that the posts impede the motion of the DNA, which requires that $\alpha > 1$, where the trivial limit $\alpha \to 1$ corresponds to the case where the posts offer no resistance whatsoever to the DNA motion.

The dispersion calculation is not performed on basic graph of Fig. 2(a), but rather on the ''local'' graph, Γ_l. The local graph, depicted in Fig. 2(b), is constructed by combining the homologous vertices outside the unit cell with their counterparts inside the unit cell. In the present circumstances, this results in loops on the local graph which correspond to consecutive hits or misses.

B. Calculation of $\overline{U}^*$ and $\overline{D}^*$

For the one-dimensional transport problem considered here, the calculation scheme requires first computing two node-based fields, $P_0^\infty(i)$ and $B(i)$, which are subsequently employed in edge-based summations which ultimately furnish $\overline{U}^*$ and $\overline{D}^*$. The field $P_0^\infty(i)$, representing the

asymptotic probability of locating the DNA at a given node i on the local graph, is computed by the solution of the equation set [14]

$$\sum_{j\in\Omega^+(i)} w(j)P_0^\infty(i')-[1-w(i)]P_0^\infty(i)=0, \tag{3.3}$$

subject to the normalization condition

$$P_0^\infty(h)+P_0^\infty(m)=1. \tag{3.4}$$

In the former, $\Omega^+(i)$ are the edges entering node i from i'. The solution of Eqs. (3.3) and (3.4) is

$$P_0^\infty(m)=\frac{1-\Pi_c}{1+\Pi_c(\alpha-1)},\quad P_0^\infty(h)=\frac{\alpha\Pi_c}{1+\Pi_c(\alpha-1)}. \tag{3.5}$$

The mean velocity is then computed by the edge sum [14],

$$\overline{U}^*=\frac{a}{T}\sum_j w(j)P_0^\infty(i'), \tag{3.6}$$

over all edges with initial vertices at i'. Use of Eq. (3.5) in the latter furnishes the mean velocity

$$\overline{U}^*=\frac{U}{1+\Pi_c(\alpha-1)}. \tag{3.7}$$

This result was anticipated in Eq. (1.1), with the retardation K being the product of the probability of hitting a post in the array Π_c and the additional time $\alpha-1$ necessary to negotiate the post.

Computation of the B field necessitates solving the equation set [14]

$$\sum_{j\in\Omega^+(i)}\left[\frac{w(j)}{T}\right]P_0^\infty(i')[B(i')+a]-\left[\frac{1-w(i)}{T}\right]P_0^\infty(i)B(i) = P_0^\infty(i)\overline{U}^*, \tag{3.8}$$

where $B(i)$ are determined to within an arbitrary additive constant. This constant can be used to set $B(h)=0$, whereupon we recover the result

$$B(m)=\frac{a-\overline{U}^*T}{\Pi_c}. \tag{3.9}$$

The dispersivity may then be computed from the edge summation [14]

$$\overline{D}^*=\frac{1}{2}\sum_j\left[\frac{w(j)}{T}\right]P_0^\infty(i')\tilde{b}(j)^2-\frac{T}{2}\overline{U}^*\overline{U}^*, \tag{3.10}$$

where $\tilde{b}(j)=a-B(i)+B(i')$ for an edge directed from i' to i. With some algebra, we arrive at

$$\frac{\overline{D}^*}{Ua}=\frac{\Pi_c(\alpha-1)[1+(2-\Pi_c)(\alpha-1)]}{2[1+\Pi_c(\alpha-1)]^3}. \tag{3.11}$$

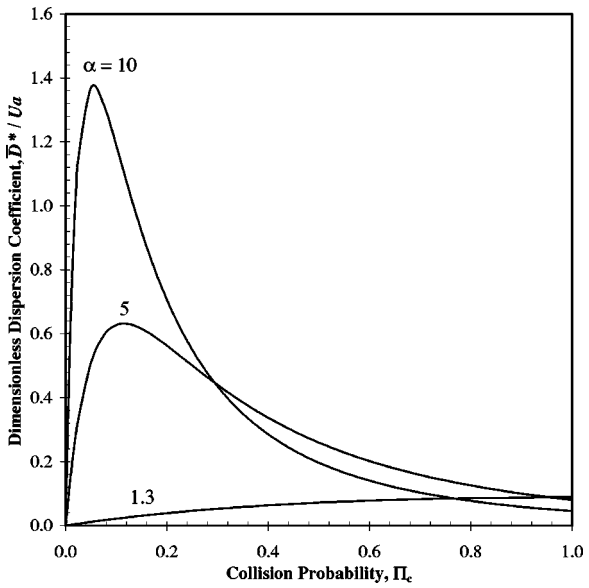

FIG. 3. Plot of the dimensionless dispersion coefficient as a function of the collision probability for the values of α indicated in the figure.

Knowledge of $\overline{U}^*$ and $\overline{D}^*$ for two different DNA permits computing the separation resolution between them over a separation length L. With the number of theoretical plates [18],

$$N=\frac{\overline{U}^*L}{2\overline{D}^*}, \tag{3.12}$$

for each species, the separation resolution is computed by [18]

$$R_s=\frac{\Delta\overline{U}^*}{\langle\overline{U}^*\rangle}\sqrt{\frac{\langle N\rangle}{16}}, \tag{3.13}$$

where Δ refers to the (positive) difference between the speeds and $\langle\cdots\rangle$ is an average value.

IV. DISCUSSION

In Fig. 3, we plot the dimensionless dispersivity of Eq. (3.11) as a function of the collision probability for several different values of α. The shapes of these curves arise from the relative contributions of the two driving forces for dispersion, namely, the stochastic hooking time, embodied in τ (and α), and the collision probability. The qualitative behavior of these curves can be most easily understood by considering three limiting cases:

(a) *Short trapping times* ($\alpha-1\ll1$). This first case, where the posts act like a sieve and offer minimal resistance to DNA motion through the array, can arise in two very different circumstances. First, short DNA tend to quickly roll off the posts without becoming strongly extended [7], an obvious case of short trapping times. For longer DNA, however, the coupling between the field strength and obstacle spacing may make the time between collisions insufficient for the

DNA to relax completely. In the latter case, the DNA is in a relatively extended state when it engages the next post, and it is unnecessary for it to complete a full ''hook-and-pulley'' mechanism before disengaging from the post, resulting again in short trapping times.

In the limit $\alpha-1\ll 1$, Eq. (3.10) possesses the leading order behavior

$$\frac{\overline{D}^*}{Ua}\approx\frac{\Pi_c}{2}(\alpha-1). \tag{4.1}$$

The dispersion is linear in Π_c, since more sieving collisions result in greater spreading, and the magnitude of the dimensionless dispersion is small because these collisions do not strongly effect the DNA mobility. Although Eq. (4.1) is only strictly valid for $\alpha-1\ll 1$, we can (arbitrarily) define and upper bound to this sieving behavior as the critical value, $\alpha^*=4/3$, whose maximum dispersion occurs at $\Pi_c=1$ [19]. There is a qualitative change in the dependence of $\overline{D}^*$ upon Π_c when $\alpha>\alpha^*$.

(b) *Long trapping times and high collision probabilities* $[\alpha-1\gg 1,\Pi_c=\mathcal{O}(1)]$. The second case can be considered the ''normal'' mode of operation for these systems. The engagement with the posts is sufficiently long to strongly effect the DNA mobility, and the number of these collisions is significant. To leading order, we now have

$$\frac{\overline{D}^*}{Ua}\approx\frac{2-\Pi_c}{2\Pi_c^2(\alpha-1)}. \tag{4.2}$$

The qualitative behavior is exactly the opposite of case (i); the dispersion now decreases with increasing Π_c or α. To understand this result, it is easiest to consider initially the case where $\Pi_c=1$. Every pass through the post region results in a collision, so the randomness in Π_c is eliminated and the dispersion is governed solely by the distribution of trapping times. The spreading between two DNA which enter a post region at the same time and are retained for respective times τ_1 and τ_2 depends upon the difference $|\tau_1-\tau_2|$, which is itself governed by the distribution of possible choices for τ_1 and τ_2. Our use of a mean trapping time τ, rather than specifying a detailed distribution, implies that the distribution of trapping times decays exponentially at the rate τ, consistent with numerical simulations [3]. Consequently, the distribution becomes ever wider as τ is decreased, and since it is this width which dominates the dispersion when $\Pi_c=1$, then $\overline{D}^*$ must increase as τ is decreased. Moreover, as the collision probability moves away from $\Pi_c=1$, $\overline{D}^*$ must increase as well, since the randomness in the trapping is now augmented by the randomness in the collision probability.

(c) *Long trapping times and low collision probabilities* $[\alpha-1\gg 1,\Pi_c(\alpha-1)\ll 1]$. The behavior in this final limit is best understood by starting at $\Pi_c=0$. This is a trivial case, since there are no collisions and the dispersion vanishes (since molecular diffusion has been neglected). As Π_c increases, to leading order

$$\frac{\overline{D}^*}{Ua}\approx\Pi_c(\alpha-1)^2. \tag{4.3}$$

The dispersion increases with increasing τ, contrary to the behavior in the opposite limit $\Pi_c=\mathcal{O}(1)$. In the small Π_c limit, the dispersion is not dominated by the distribution of trapping times, but rather by the magnitude of τ. Returning to our example of two DNA with trapping times τ_1 and τ_2, it is very likely in the low Π_c limit that one of the DNA, say number 2, will not be trapped at all. In this case, its trapping time vanishes, $\tau_2=0$, and it is the magnitude of τ_1, rather than the distribution governing τ_1, which determines the difference in the ''trapping'' times and the spreading [21]. The large contribution to $\overline{D}^*$ from the trapping time in the low Π_c (dilute array) limit is consistent with detailed single-post numerical simulations [4].

Having analyzed the limiting behavior of $\overline{D}^*$, we now turn our attention to estimating $\overline{D}^*$ in Ephesia experiments. Explicitly, for the separation of λ-phage DNA and its dimer [15], collision probabilities of $\Pi_c\approx 0.35$ and trapping times of $\alpha\approx 2-5$ were observed, which indicates that the dispersion should be somewhere between cases (ii) and (iii). From Eq. (3.11) (or, alternatively, Fig. 3), the dimensionless dispersion coefficient is typically between 0.1 and 0.5. Using the values cited in Sec. II and a nominal electric field strength of 10 V/cm, we estimate that the dispersivity induced by the presence of the posts is typically 60-300 times greater than molecular diffusion alone. This is consistent with both the underlying assumption in this analysis, namely, that the dispersion is dominated by the post interactions, and the situation encountered in experiments.

In addition to making the latter numerical estimates, significant insights into $\overline{D}^*$ and the separation resolution can be obtained by adopting simple models for τ and Π_c. To this extent, we will assume that $\tau\sim E^{-1}$ and $\Pi_c\sim d/a$. In such a model, α and Π_c are no longer functions of E, whereupon we recover the scaling $\overline{D}^*\sim E$. This is analogous to classical results for the dispersion of tracer particles in strong flow through porous media [20], where the dispersion is linear with the flow strength. Moreover, since $\overline{D}^*$ and $\overline{U}^*$ are linear in E, then number of plates N and the separation resolution R_s are independent of E. As a consequence, a plot of the separation resolution against the electric field would plateau at high field strengths. Given a fixed chip size L, the overall efficiency is optimized by running at higher fields, since the separation time is decreased without sacrificing resolution. Likewise, for a given separation time $L/\langle\overline{U}^*\rangle$ (or, equivalently, a given ratio L/E), the separation resolution is optimized by employing large values of L and E, in accord with experiments [15]. In light of the fact that $\tau\sim E^{-1}$ and $\Pi_c\sim a/d$ are only rough approximations, the latter observations should be viewed as general trends, rather than quantitative statements.

V. CONCLUSION

In the present contribution, we have presented a straightforward semiphenomenological model for DNA separation

in the arrays of posts typical of self-assembled magnetic particles. For the most part, we have treated the trapping time and collision probability as parameters in a coarse-grained model, rather than specifying a more detailed scheme for their quantification as a function of the DNA size, electric field, post geometry, etc. The analytical simplicity of our results allowed us to readily identify different regimes in the dispersivity, as well as furnish order of magnitude estimates for the dispersion and separation resolution and predict optimal operating conditions.

At first glance, our approach may appear overly simplistic, since we have not explicitly accounted for any molecular phenomena. Nevertheless, our results have captured many of the trends observed in both numerical simulations and experiments. Consequently, the overall character of these trends probably owes more to the inherent randomness in the collision frequency and duration, rather than the exact details of the statistics and their molecular underpinning. However, moving from qualitative observations to quantitative predictions necessitates choosing a particular model for the post interactions. Although the existing models are probably too limited to accurately capture the relevant experimental data [15], it is inevitable that detailed experimental [16] and numerical data will eventually become available. We anticipate that the synthesis of the latter data with the present theory, when verified by further experimental data on separations in real arrays [15], will ultimately lead to a greater understanding of this separation process and its optimization.

ACKNOWLEDGMENTS

We are grateful to Professor Patrick S. Doyle and Greg Randall at MIT for sharing unpublished experimental results on single-post dynamics, and Nicolas Minc at Institut Curie for useful discussions. This work was supported by the Human Frontier Science Program and the Nanostructures/Nanosciences Program from the French Department of Research.

[1] W.D. Volkmuth and R.H. Austin, Nature (London) **358**, 600 (1992).
[2] W.D. Volkmuth, T. Duke, M.C. Wu, R.H. Austin, and A. Szabo, Phys. Rev. Lett. **72**, 2117 (1994).
[3] E.M. Sevick and D.R.M. Williams, Phys. Rev. E **50**, R3357 (1994).
[4] G.I. Nixon and G.W. Slater, Phys. Rev. E **50**, 5033 (1994).
[5] E.M. Sevick and D.R.M. Williams, Phys. Rev. Lett. **76**, 2595 (1996).
[6] P. André, D. Long, and A. Ajdari, Eur. Phys. J. B **4**, 307 (1998).
[7] P.M. Saville and E.M. Sevick, Macromolecules **32**, 892 (1999).
[8] P.D. Patel and E.S.G. Shaqfeh, J. Chem. Phys. **118**, 2941 (2003).
[9] P.S. Doyle, J. Bibette, A. Bancaud, and J.-L. Viovy, Science **295**, 2237 (2002).
[10] D. Ertas, Phys. Rev. Lett. **80**, 1548 (1998).
[11] T.A.J. Duke and R.H. Austin, Phys. Rev. Lett. **80**, 1552 (1998).
[12] J. Han, S.W. Turner, and H.G. Craighead, Phys. Rev. Lett. **83**, 1688 (1999).
[13] K.D. Dorfman, J. Chem. Phys. **118**, 8428 (2003).
[14] K.D. Dorfman, G.W. Slater, and M.G. Gauthier, J. Chem. Phys. **119**, 6979 (2003).
[15] N. Minc, C. Fütterer, C. Gosse, K. D. Dorfman, and J.-L. Viovy, in *Proceedings of the Seventh International Conference on Miniaturized Chemical and BioChemical Analysis Systems*, edited by M.A. Northrup, K.F. Jensen, and D.J. Harrison (The Transducers Research Foundation, Squaw Valley, CA, 2003); N. Minc, K. D. Dorfman, C. Fütterer, C. Gosse, C. Goubault, and J.-L. Viovy (unpublished).
[16] P. S. Doyle and G. Randall (private communication).
[17] M.G. Gauthier and G.W. Slater, J. Chem. Phys. **117**, 6745 (2002).
[18] J. C. Giddings, *Unified Separation Science* (Wiley, New York, 1991).
[19] For $\alpha<\alpha^*$, $\bar{D}^*$ has a maximum at aphysical values of $\Pi_c>1$.
[20] J. Bear, *Dynamics of Fluids in Porous Media* (Elsevier, New York, 1972).
[21] An alternative way to view this limit is to include the misses in the distribution for τ_1, whereupon the distribution would be strongly peaked at both zero and the mean value.